Journal of Sol-Gel Science and Technology (2018) 87:676–684
https://doi.org/10.1007/s10971-018-4760-5

ORIGINAL PAPER: SOL-GEL AND HYBRID MATERIALS FOR CATALYTIC, PHOTOELECTROCHEMICAL AND SENSOR APPLICATIONS

Effect of pretreatment on microstructure and photocatalytic activity of kaolinite/TiO_2 composite

Hongliang Xu[1] · Shiping Sun[1] · Sanying Jiang[1,2] · Hailong Wang[1] · Rui Zhang[1,3] · Qinfu Liu[4]

Received: 1 May 2018 / Accepted: 23 July 2018 / Published online: 30 July 2018

Abstract

Kaolinite/TiO_2 composites were prepared by using sol-gel method and raw kaolin, pretreated kaolinite and tetrabutyl titanate as the main raw materials. X-ray diffractometer, field-emission scanning electron microscope and infrared spectrometer analysis were carried out to characterize the phase composition and microstructure of the samples. The photocatalytic performance of the kaolinite/TiO_2 composites were evaluated by degrading the methylene blue (MB) and phenol aqueous solution, respectively. The results show that intercalation and exfoliation reduced the size and thickness of kaolinite particles. Acid treatment improved the distribution and the loading quantity of TiO_2 grains. When the kaolinite/TiO_2 composites were calcined at 500 °C, the tetragonal structure of anatase particles of 30–100 nm in size were obtained, but the exfoliated kaolinite crystals were damaged. The degradation rate of MB increased gradually with the extension of photocatalytic reaction time and the enhancement of photocatalyst dosage. The adsorption performance of acid-treated kaolinite/TiO_2 composite (AKT) was nearly the same as that of raw kaolin/TiO_2 composite (RKT), but that of the exfoliated kaolinite/TiO_2 composite (EKT) was the most excellent. The photocatalytic performance of AKT and EKT were better than that of RKT, and AKT exhibited the optimum property. Under a certain photocatalyst dosage and photocatalysis time, the absorption rate and the degradation rate decreased gradually with the enhancement of initial concentration of MB. Similar result was also acquired for the degradation of phenol. Both the acid treating and the exfoliating to kaolinite enhanced the photocatalytic performance of the kaolinite/TiO_2 composite photocatalysts, but acid treatment may be more helpful to the preparation of high performance kaolinite/TiO_2 composite photocatalyst.

Graphical Abstract

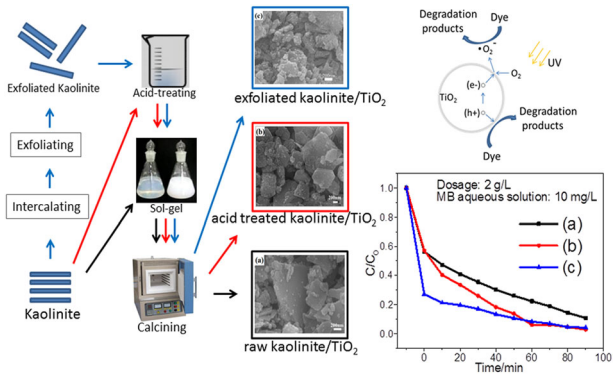

Pretreatment of kaolinite improved the microstructure and photocatalytic performance of kaolinite/TiO_2 composites.

✉ Hongliang Xu
xhlxhl@zzu.edu.cn

[1] School of Materials Science and Engineering, Zhengzhou University, 450001 Zhengzhou, China

[2] Beijing New Voyaging Co., Ltd., 101118 Beijing, China

[3] Zhengzhou University of Aeronautics, 450015 Zhengzhou, China

[4] College of Geoscience and Surveying Engineering, China University of Mining and Technology, 100083 Beijing, China

Highlights

- Natural kaolinite particles were pretreated by acid treating or intercalating-exfoliating.
- Kaolinite/TiO_2 composites were prepared by sol-gel method.
- Pretreatment of kaolinite improved the photocatalytic performance of kaolinite/TiO_2 composite.

Keywords Kaolinite · Pretreatment · Kaolinite/TiO_2 composite · Photocatalytic activity

1 Introduction

Nowadays, environmental pollution becomes a serious and urgent problem challenging the sustainable development of human society. Large quantities of wastewater was always discharged into the aquatic environment without effective treatments and then seriously harmed the environment [1], such as the dye wastewater [2]. Traditional methods of wastewater treatment, such as coagulating sedimentation, filtration and adsorption, have some disadvantages and are ineffective sometimes for removing the dyes [3]. As a new kind of technology, photocatalytic method has been used to treat wastewater and has attracted extensive attention recently [4, 5]. Photocatalyst [6, 7], which is the key of photocatalytic technology, has become a hot topic in the field of materials research. Although a wide variety of photocatalysts have been explored, most of them are not applied in large scale [8]. Up to now, TiO_2 is the common used photocatalysis [9, 10] due to the low cost, chemical stability and nontoxicity. Nano-TiO_2 grains exhibited excellent photocatalytic performance in degrading organic dyes in wastewater [11]. However, single nano-TiO_2 particle was easily agglomerated and then weakened the photocatalytic efficiency. On the other hand, it is difficult to separate and recycle the nano-TiO_2 particles from water after the photocatalytic process. Therefore, nano-TiO_2 particles were usually dispersed and immobilized on the carriers [12–14].

A suitable carrier for TiO_2 photocatalyst should possess following characteristics such as good light transmission [15], strong binding force with TiO_2 particles without affecting the photocatalytic activity, large specific surface area and strong adsorption capacity for organic contaminants [16]. Due to the low cost, clay minerals were investigated as photocatalysts carrier by many researchers [11–13, 17–22]. The specific surface area is important for the adsorption capacity of clay minerals and the photocatalytic properties of the clay/TiO_2 composites [23, 24]. For all the clay mineral carriers, montmorillonite has excellent absorption capacity as it is a natural nano material. Although kaolinite is rich in reserves, natural kaolinite always has large size, small specific area and contaminated surface. These phenomena lead to not only the low adsorption capacity of kaolinite, but also the low loading ratio of TiO_2 in kaolinite/TiO_2 composite, as well as the weak bonding force between TiO_2 and kaolinite, which are the disadvantages for the photocatalytic performances of kaolinite/TiO_2 composites. As a result, many works should be carried out in the future.

Nanoscale kaolinites [25–27] with a high specific surface area and better adsorption capacity, can be prepared by intercalation [28] and exfoliation method [29, 30]. On the other hand, the surface of kaolinite was cleaned and activated by acid treatment [31–33] in order to improve the reaction activity. However, there is little report about the influence of acid treating or intercalating/exfoliating of natural kaolinite on the photocatalytic activity of kaolinite/TiO_2 composite up to now. Consequently, natural kaolin was pretreated by acid treating or intercalating/exfoliating firstly in this study. Then, kaolinite/TiO_2 composites were prepared by using sol-gel method and tetrabutyl titanate as the TiO_2 precursor. The degradation rates of methylene blue (MB), a commonly used dye, as well as phenol by kaolinite/TiO_2 composites were measured for evaluating the effects of pretreatment on the photocatalytic performance of kaolinite/TiO_2 composite.

2 Experimental

2.1 Materials

Raw kaolin (RK) used in this study was a natural kaolin collected from a mine in Zhangjiakou, China, with a particle size smaller than 45 μm. As the molar ratio of SiO_2/Al_2O_3 (2.02) of RK was close to the theory value of kaolinite (2.0), it can be inferred that RK contained mainly kaolinite, and a small amount of impurity minerals, such as quartz.

Anhydrous ethanol (C_2H_5OH), potassium acetate (KAc), glacial acetic acid (HAc), concentrated hydrochloric acid (HCl) and MB ($C_{16}H_{18}ClN_3S$) were analytical reagents, butyl-titanate ($Ti(OC_4H_9)_4$) was chemically pure, and the deionized water was used in this study.

2.2 Pretreatment of kaolin

A certain amount of RK was added into the 4 mol L^{-1} HCl solution and stirred magnetically at 25 °C for 3 h, followed by washing with deionized water, centrifuging separation and drying, then obtained the acid-treated kaolin (AK).

Together with an appropriate amount of deionized water, RK and KAc (with a weight ratio of 1:1) were ground in agate mortar to get paste, then aged for 24 h to fulfill the intercalation of KAc molecules into kaolinite. Exfoliation of kaolinite was realized by washing the kaolinte/KAc intercalation compounds with anhydrous alcohol, followed by ultrasonic processing, centrifuging and drying. The as-obtained powder was carried out for other two cycles of intercalating and exfoliating process. Finally, the obtained powder was acid treated according to the method stated above to acquire the exfoliated kaolin (EK).

2.3 Preparation of kaolinite/TiO_2 composites

Sol-gel method was performed to synthesize the precursor of TiO_2, which composed of $Ti(OC_4H_9)_4$, C_2H_5OH, H_2O and HAc with a molar ratio of 1:32:2:0.9. In details, 2/3 of C_2H_5OH was magnetically stirred for 30 min with $Ti(OC_4H_9)_4$ and HAc, followed by adding the mixture of deionized water and the remaining 1/3 of C_2H_5OH, adjusting the pH value to 3, then magnetic stirring for 60 min and ultrasonic treating for 10 min. Thus obtained the transparent yellowish sol of TiO_2 precursor.

Based on our previous study, the kaolinite/TiO_2 composite was designed with a ratio of TiO_2 to kaolinite of 5 mmol g^{-1}. A certain concentration of RK suspension was prepared firstly. Then, a proper amount of TiO_2 precursor was dropped into the vigorously stirred RK suspension. After stirring for 3 h, the mixture was aged at room temperature for 24 h and then fully dried at 70 °C. Subsequently, the as-acquired solid mixture was calcined at 500 °C for 2 h to obtain the kaolinite/TiO_2 composite (RKT).

Using the same method, kaolinite/TiO_2 composites can also be prepared by using AK and EK, which were denoted as AKT and EKT, respectively.

2.4 Characterization techniques

The crystalline structure was investigated by an X-ray diffractometer (XD-3, Beijing Purkinje General Instrument Co., Ltd., China) with Cu Kα radiation ($\lambda = 1.5406$ Å) and scanning rate of 4° min^{-1} at 36 kV, 20 mA. The microstructure was observed by a field-emission scanning electron microscope (SEM, Quanta FEG 250, FEI Co., Ltd, Portland, USA). The chemical functional groups were determined by an infrared spectrometer (Nicolet iS10, Thermo Fisher Scientific Corp., Massachusetts, USA) with the scanning range of 4000–400 cm^{-1} and resolution of 4 cm^{-1}. Ultra violet (UV)-visible spectrum was performed by the use of an UV-visible spectrometer (UV-1800PC, Shanghai United States spectrum of Instrument Co., Ltd, China) with the scanning range of 800–400 cm^{-1} and resolution of 1 cm^{-1}.

2.5 Measurement of photocatalytic activity

The photocatalytic performance of the composites was evaluated by the degradation rate of MB solution. The light source was a 250 W high pressure mercury lamp whose main wavelength was 365 nm, and the height from the mercury lamp to the reaction level was 15 cm. The entire photocatalytic degradation experiment was carried out at room temperature in a self-made photocatalytic reaction vessel. A certain amount of kaolinite/TiO_2 composite powder was added into a 100 mL aqueous solution of MB. Prior to irradiation, the adsorption–desorption equilibrium reaction was achieved firstly in the dark box for 1 h. Then the suspension was irradiated and sampled at regular intervals. The supernatant MB solution not containing the solid particles of the catalyst was packed in a beaker and the residual absorbance curve of the MB solution was measured by UV-1800PC UV-Vis spectrophotometer after 5 ml liquid samples were centrifuged (7000 r min^{-1}, 4 min). The absorbance at 665 nm of the characteristic wavelength of the maximum absorption peak of MB was used to determine the concentration of aqueous MB. According to the initial absorbance of MB solution and the residual absorbance of MB solution after different time, the removal rate of composite materials on MB can be calculated. Using the similar method, phenol was used to evaluate the photocatalytic activity of kaolinite/TiO_2 to the colorless organic pollutant. The absorbance at 270 nm of the maximum absorption peak of phenol was used to determine the concentration of phenol aqueous solution.

3 Results and discussion

3.1 Phase analysis

Figure 1 presents the X-ray diffraction (XRD) patterns of RK, AK and EK. It can be seen clearly that RK consisted mainly of kaolinite and a small quantity of quartz (Fig. 1a). AK had the similar XRD pattern (Fig. 1b) as that of RK, indicating that acid treatment did not damage the crystal structure of kaolinite. All the diffraction peaks of kaolinite still appeared on the XRD pattern of EK (Fig. 1c). However, they were broadened significantly and weakened a little compared with those on the patterns of RK and AK, such as (001) and (002). This phenomenon suggests that the crystallinity and grain size of kaolinite were reduced after three cycles of intercalation and exfoliation.

Figure 2 shows the XRD patterns of RKT, AKT and EKT. Patterns of all the three samples had typical diffraction peaks of anatase at 2θ of about 25.3, 48.2, 54.2, 55.1 and 62.9°, which are assigned to (101), (200), (105), (211) and (204), respectively. Rietveld refinement confirms the

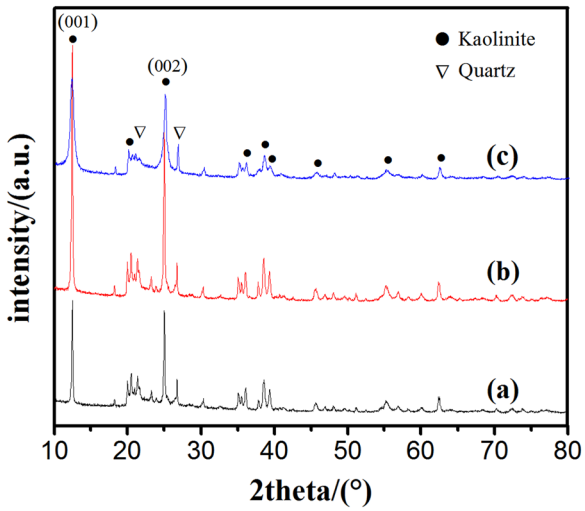

Fig. 1 XRD patterns of kaolin and pretreated kaolin. **a** RK; **b** AK; **c** EK

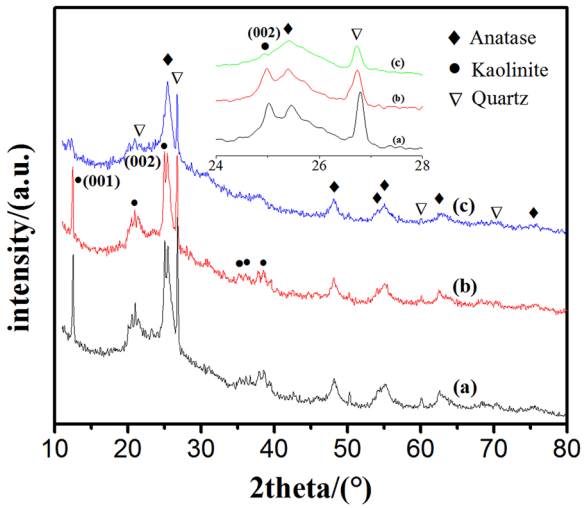

Fig. 2 XRD patterns of kaolinite/TiO_2 composites. **a** RKT; **b** AKT; **c** EKT

tetragonal structure of anatase in as-obtained kaolinite/TiO_2 samples. For example, the unit cell parameters of anatase in RKT are $a = 0.343$ nm, $b = 0.343$ nm, $c = 2.09$ nm, respectively. No peaks of rutile were observed. This result indicates that the TiO_2 precursor was only transformed to anatase when calcined at 500 °C. The diffraction peaks of kaolinite still appeared on the patterns of RKT and AKT, but the relative intensity of I_{001} of kaolinte to I_{100} of quartz decreased slightly compared with those of RK and AK (Figs. 1 and 2). Obviously, a small amount of kaolinite were damaged but most of them were unaffected when RKT and AKT had been calcined at 500 °C.

However, diffraction peaks (001) and (002) of kaolinite almost disappeared on the XRD pattern of EKT, indicating that nearly all kaolinite crystals were damaged when EKT was calcined at 500 °C. This result is ascribed to the dehydroxylation of kaolinite [11]. It can be concluded that the dehydration temperature dropped as the grain size of kaolinite reduced by intercalating and exfoliating, which is coincide with the previous reports [34], and the hydroxyl was removed easily after calcination at 500 °C. Therefore, it can be assumed that hydroxyl of kaolinite was eliminated more easily after exfoliating treatment. Obviously, the dehydration of kaolinite would obtain microporous particles, which was helpful to the absorption property.

3.2 Microstructural analysis

Figure 3 exhibits SEM images of the pretreated kaolinite and the as-prepared kaolinite/TiO_2 composite samples. Kaolinite particles in RK presented a typical pseudo-hexagonal shape, lamellar structure and a grain size smaller than 3 μm (Fig. 3a). Kaolinite crystals in AK had the same shape and size as those in RK (Fig. 3b). Kaolinite in EK possessed the same shape as those in RK (Fig. 3c). However, the grain size and thickness of kaolinite particles decreased significantly compared with those of RK and AK, in line with the XRD analysis. This result is also ascribed to the three cycles of intercalation and exfoliation treatment of kaolinite.

All the three samples RKT, AKT and EKT were loaded with TiO_2 particles of 10–30 nm in size (Figs. 3d-f), which was also confirmed by the energy dispersive spectrometer (EDS) and XRD analysis (Fig. 2). For RKT, TiO_2 grains were mostly distributed at the corner or edge of kaolinite crystals, but seldom loaded on the surface. This phenomenon was similar to the report of Kutláková et al. [11], indicating that the smooth surface of kaolinite was not suitable for the growth of TiO_2 grains.

AK was loaded with larger amount of TiO_2 grains compared with RK, and TiO_2 grains were uniformly distributed on the kaolinite surface. The main reason for this phenomenon may be due to the removing of impurities and the introducing of hydroxyl on the kaolinite surface by the acid treatment. Same phenomenon can also be observed in the SEM images of EKT. In addition, it should be noted that the EKT particles kept the same morphology as RKT and AKT, although the kaolinite crystals in EKT had undergone dehydroxylation.

3.3 Infrared spectroscopy analysis

The Fourier Transform Infrared (FT-IR) spectra of kaolin and kaolinite/TiO_2 composite samples are given in Fig. 4. RK presented all the characteristic vibration bands of kaolinite (Fig. 4a). The stretching vibrations of inner-surface hydroxyls and inner hydroxyls were located at 3695, 3667, 3652 and 3620 cm^{-1}, respectively. Their bending vibrations appeared at 938 and 914 cm^{-1}, correspondingly [27]. The

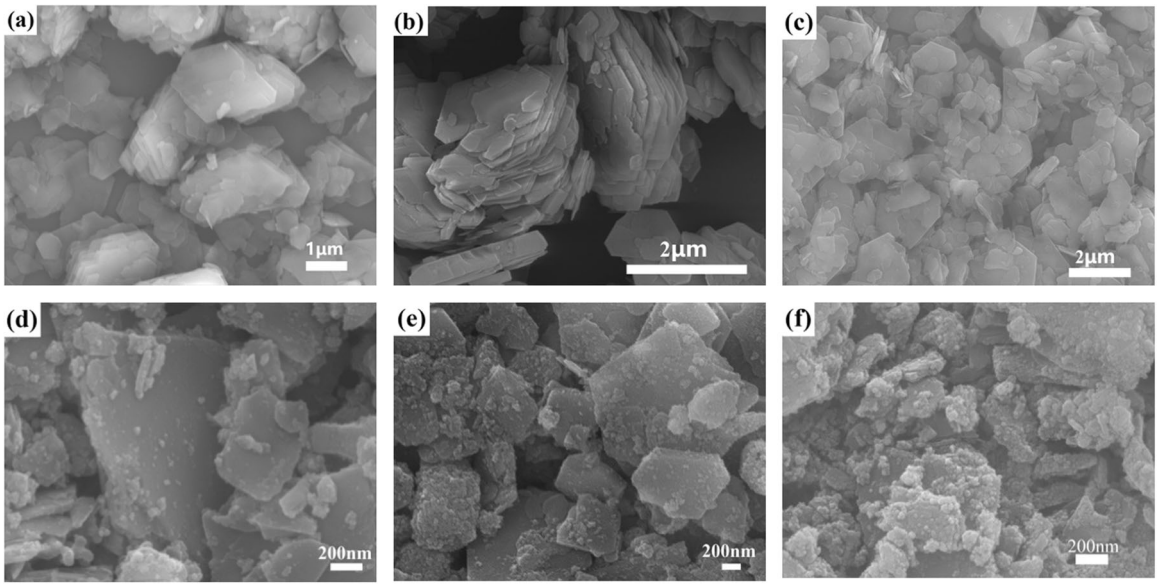

Fig. 3 SEM images of raw kaolinite, pretreated kaolinite and kaolinite/TiO_2 composites. **a** RK; **b** AK; **c** EK; **d** RKT; **e** AKT; **f** EKT

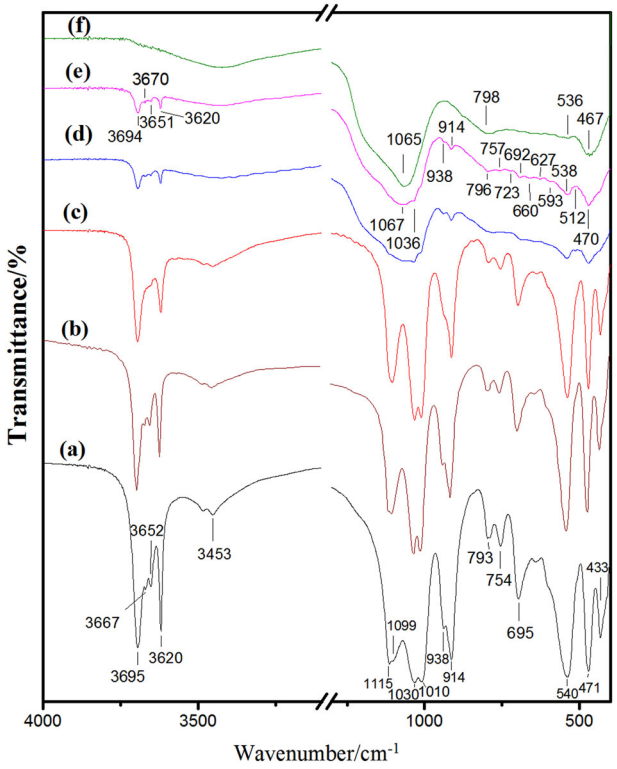

Fig. 4 Infrared spectra of kaolinite and kaolinite/TiO_2 composites. **a** RK; **b** AK; **c** EK; **d** RKT; **e** AKT; **f** EKT

bands at 1115, 1030, 1010, 793 and 471 cm^{-1} are assigned to the vibrations of Si-O bonds, and bands at 754, 695 and 540 cm^{-1} are attributed to vibrations of Si-O-Al bonds [11]. The band at 3453 cm^{-1} is ascribed to the stretching vibration of water molecules adsorbed on the external surface of kaolinite [35, 36]. AK and EK had the similar FT-IR spectra as RK did, except for the weakening of bands at 3667 and 3652 cm^{-1} on the spectrum of EK.

For the FT-IR spectra of RKT, AKT and EKT, the broad band at about 1060 cm^{-1} and the bands in the regions of 660–550 cm^{-1}, 470–436 cm^{-1} are ascribed to the vibrations of Ti-O-H, Ti-O and Ti-O-Ti bonds, respectively, indicating that these composite samples did contain TiO_2 grains [11, 37]. It should be noted that the transmittance of bands at 3620–3695 cm^{-1} reduced significantly for RKT and AKT, and even disappeared for EKT. These phenomena coincides with the result of XRD analysis that some kaolinite in RKT and AKT were dehydrated and nearly all the kaolinite in EKT were dehydrated.

In view of the analysis of XRD, SEM and FT-IR, it can be inferred that TiO_2 precursor was coated on the surface of kaolinite by the sol-gel method. Acid treating of kaolinite make the TiO_2 precursor cover more uniformly and attach more tightly on the surface of kaolinite crystals. When calcined at 500 °C, the TiO_2 precursor was converted to anatase and kaolinite crystals were kept undamaged for the RKT and AKT, but damaged for the EKT sample.

3.4 Photocatalytic activity of kaolinte/TiO_2 composites

3.4.1 Effect of photocatalyst dosage on the photocatalytic performance

Figure 5 exhibits the degradation curves of MB aqueous solution (10 mg L^{-1}) by the different dosage of kaolinte/TiO_2 composite. The degradation rate of MB increased gradually with the extension of photocatalytic reaction time

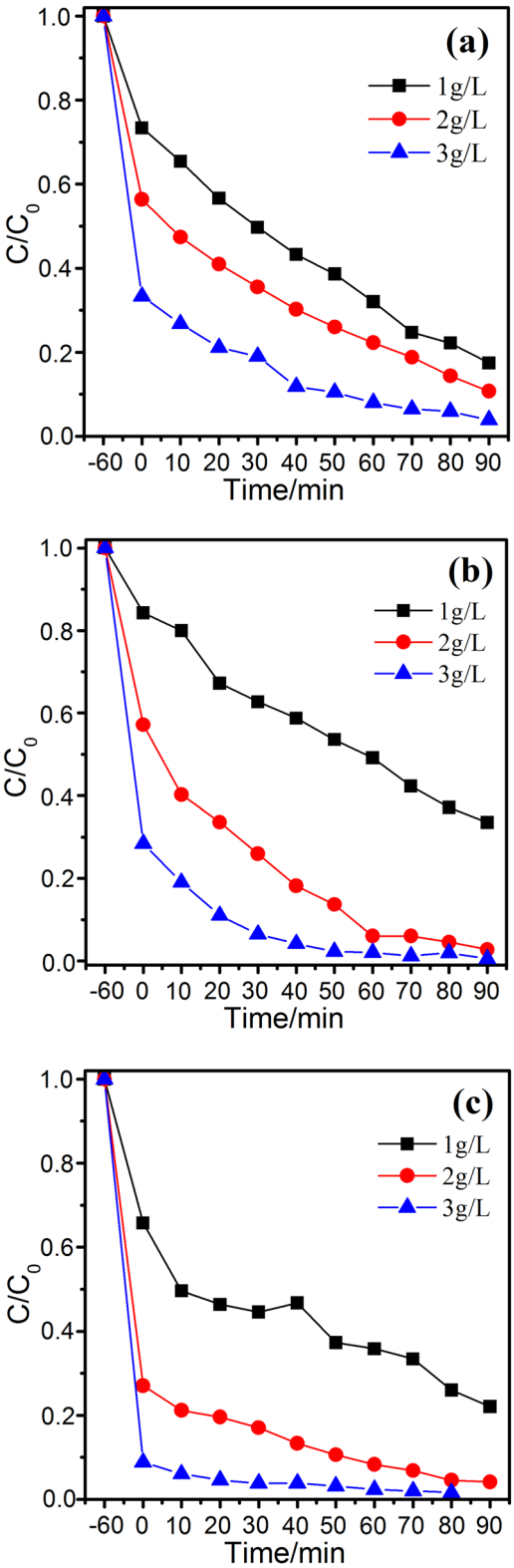

Fig. 5 Degradation curves of MB solution by different dosages of kaolinite/TiO_2 composites. **a** RKT; **b** AKT; **c** EKT

and the enhancement of photocatalyst dosage. For example, when the RKT dosage was 2 g L^{-1}, the degradation rate of MB reached 73.97 and 89.26% after photocatalysis for 50 and 90 min, respectively. When photocatalysis for 90 min, the degradation rate increased from 82.56% through 89.26 to 96.06% with the dosage rising from 1 to 2 g L^{-1}, 3 g L^{-1}, correspondingly.

It should be pointed out that the degradation rate of MB during the dark reaction period was indeed derived from the absorption of photocatalyst. The adsorption performance of AKT was nearly the same as that of RKT, but EKT showed the most excellent adsorption performance among the three samples. For instance, the degradation rate during dark reaction period achieved 43.61, 42.84 and 72.93% by inputting 2 g L^{-1} of RKT, AKT and EKT, respectively. This result is mainly ascribed to the reduced particle size of kaolinite in EK by the intercalating and exfoliating treatment, as well as the dehydration of kaolinite in EKT during the calcination process.

The photocatalytic performance of AKT and EKT were better than that of RKT, and AKT exhibited the optimum property. With the photocatalyst dosage of 2 g L^{-1} and photocatalysis for 60 min, the degradation rates of MB by RKT, AKT and EKT achieved 77.71%, 93.94% and 91.68%, respectively. In addition, for AKT and EKT, the degradation rate of MB by the dosage of 2 g L^{-1} approached to that of 3 g L^{-1} as the photocatalysis time rising up to 90 min. As a result, AKT was the optimum photocatalyst and 2 g L^{-1} would be the optimum dosage.

3.4.2 Effect of initial concentration of MB solution on the photocatalytic performance

Figure 6 shows the degradation curves of MB solutions with different initial concentration by inputting 2 g L^{-1} kaolinite/TiO_2 composites. Under a certain photocatalyst dosage and photocatalysis time, the absorption rate and the degradation rate decreased gradually with the enhancement of initial concentration. The degradation rate of MB increased with the prolonging of photocatalysis time. No matter what the initial MB concentration was, AKT and EKT exhibited better photocatalytic activity than RKT did. It should be noted that AKT achieved the high degradation rate of 94.05% for MB solution with initial concentration of 15 mg L^{-1} when photocatalysis for 90 min, which was nearly similar to that for MB solution with initial concentration of 10 mg L^{-1}. Consequently, it can be inferred that acid treatment to RK was the best and economic pretreatment method to prepare high performance kaolinite/TiO_2 composite photocatalyst. Compared with other kaolinite/TiO_2 composite materials [38], the AKT and EKT exhibited the better photocatalytic performance, especially the adsorption performance of the EKT sample is particularly excellent.

In order to eliminate the effect of dye on the absorption of UV and visible light, phenol, a colorless organic

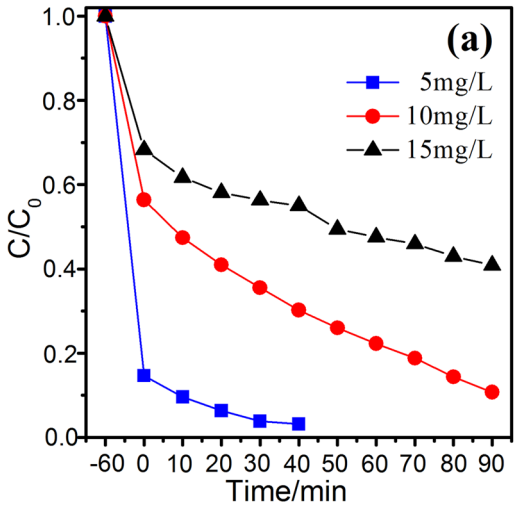

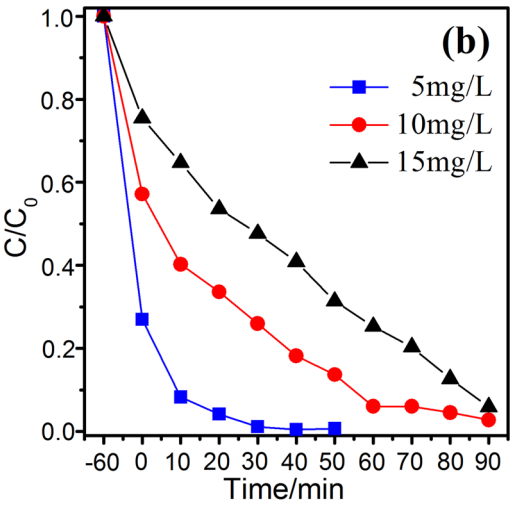

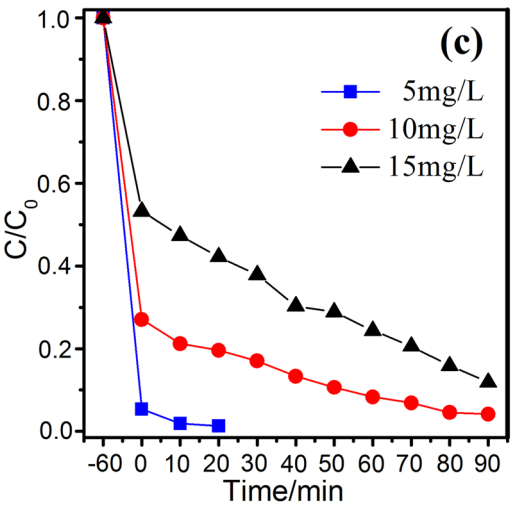

Fig. 6 Degradation curves of MB solution with different initial concentration by kaolinite/TiO_2 composites. **a** RKT; **b** AKT; **c** EKT

pollutant, was used to evaluate photocatalytic efficiency of kaolinite/TiO_2 composite. Phenol aqueous solution (10 mg

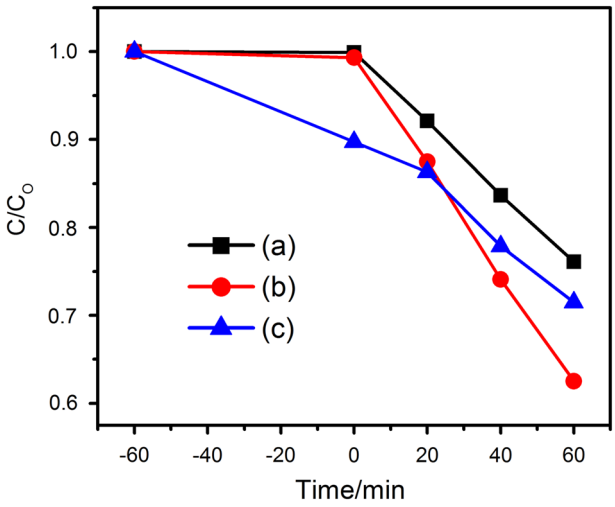

Fig. 7 Degradation curves of phenol solution by kaolinite/TiO_2 composites. **a** RKT; **b** AKT; **c** EKT

L^{-1}, 100 mL) and dosage of 200 mg photocatalyst were used in the photocatalytic experiment. Similar to the result of degradation for MB, the adsorption performance of AKT for phenol was nearly the same as that of RKT, and EKT exhibited the most excellent adsorption performance (Fig. 7). The degradation rate of phenol increased gradually with the extension of photocatalytic reaction time. When photocatalysis for 60 min, the degradation rate of phenol by RKT, AKT and EKT reached 23.5%, 37.5% and 28.5%, respectively. Obviously, these degradation rates are lower than those of MB. This result indicates that the degradation efficiency of kaolinite/TiO_2 composite on phenol was lower than that on MB.

4 Conclusion

The kaolinite/TiO_2 composite photocatalysts were prepared successfully by sol-gel method and using RK and pretreated kaolin as the carrier and tetrabutyl titanate as TiO_2 precursors, respectively. The size and thickness of EK particles decreased significantly compared with those of RK and AK. Acid treatment improved the distribution and the loading quantity of TiO_2 grains. When the kaolinite/TiO_2 composites were calcined at 500 °C, the tetragonal structure of anatase particles size of 30–100 nm in size were obtained, but the exfoliated kaolinite crystals were damaged. The degradation rate of MB increased with the enhancement of photocatalytic reaction time and photocatalyst dosage, but decreased with the rising of initial MB concentration. The photocatalytic performances of AKT and EKT were significantly better than RKT samples, and AKT exhibited the optimum property. Similar result was also acquired for the degradation of phenol. Both the acid treating and the

exfoliating to kaolinite enhanced the photocatalytic performance of the kaolinite/TiO_2 composite photocatalysts, but acid treatment may be more helpful to the preparation of high performance kaolinite/TiO_2 composite photocatalyst.

Acknowledgements This work was supported by the Key Science and Technology Research Project of Henan province, China (grant number 182102210005) and the Key Scientific Research Projects for Institutes of Higher Education of Henan Province, China (grant number 15A430010).

Compliance with ethical standards

Conflict of interest The authors declare that they have no conflict of interest.

References

1. Wang BJ, Zhu Y, Bai ZS, Luque R, Xuan J (2017) Functionalized chitosan biosorbents with ultra-high performance, mechanical strength and tunable selectivity for heavy metals in wastewater treatment. Chem Eng J 325:350–359
2. Lmb B, Dos Santos AJ, Da SD, Apm A, Garciasegura S, Martínezhuitle CA (2017) Solar photocatalytic application of NbO_2OH as alternative photocatalyst for water treatment. Sci Total Environ 596-597:79–86
3. Yang YQ, Zhang GK (2012) Preparation and photocatalytic properties of visible light driven Ag-AgBr/attapulgite nanocomposite. Appl Clay Sci 67-68:11–17
4. Wang MG, Han J, Hu YM, Guo R, Yin YD (2016) Carbon-incorporated NiO/TiO_2 mesoporous shells with p-n heterojunctions for efficient visible light photocatalysis. Acs Appl Mater Interfaces 8:29511–29521
5. Kofuji Y, Ohkita S, Shiraishi Y, Sakamoto H, Tanaka S, Ichikawa S, Hirai T (2016) Graphitic carbon nitride doped with biphenyl diimide: efficient photocatalyst for hydrogen peroxide production from water and molecular oxygen by sunlight. Acs Catal 6:7021–7029
6. Ling CC, Ye XJ, Zhang JH, Zhang JF, Zhang SJ, Meng SG, Fu XL, Chen SF (2017) Solvothermal synthesis of $CdIn_2S_4$ photocatalyst for selective photosynthesis of organic aromatic compounds under visible light. Sci Rep 7:27
7. Reli M, Huo P, Šihor M, Ambrožová N, Troppová I, Matějová L, Lang J, Svoboda L, Kuśtrowski P, Ritz M (2016) Novel TiO_2/C_3N_4 photocatalysts for photocatalytic reduction of CO_2 and for photocatalytic decomposition of N_2O. J Phys Chem A 120:8564–8573
8. Chen DM, Wang ZH, Ren TZ, Ding H, Yao WQ, Zong RL, Zhu YF (2014) Influence of defects on the photocatalytic activity of ZnO. J Phys Chem C 118:15300–15307
9. Yu HG, Xiao P, Tian J, Wang FZ, Yu JG (2016) Phenylamine-functionalized rGO/TiO_2 photocatalysts: spatially separated adsorption sites and tunable photocatalytic selectivity. Acs Appl Mater Interfaces 8:29470–29477
10. Khan H, Swati IK (2016) Fe^{3+}-doped anatase TiO_2 with d–d transition, oxygen vacancies and Ti^{3+} centers: synthesis, characterization, UV-vis photocatalytic and mechanistic studies. Ind Eng Chem Res 55:6619–6633
11. Mamulová, Kutláková K, Tokarský J, Vojtěšková S, Kovář P, Kovářová A, Smetana B, Kukutschová J, Čapková P, Matějka V (2011) Preparation and characterization of photoactive composite kaolinite/TiO_2 J Hazard Mater 188:212–220
12. Yuan LL, Huang DD, Guo WN, Yang QX, Yu J (2011) TiO_2/montmorillonite nanocomposite for removal of organic pollutant. Appl Clay Sci 53:272–278
13. Todorova N, Giannakopoulou T, Karapati S, Petridis D, Vaimakis T, Trapalis C (2014) Composite TiO_2/clays materials for photocatalytic NOx oxidation. Appl Surf Sci 319:113–120
14. Yang L, Wang FZ, Chang S, Liu P, Zhang WQ, Hu SG (2016) An in-situ synthesis of Ag/AgCl/TiO_2/hierarchical porous magnesian material and its photocatalytic performance. Sci Rep 6:21617
15. Ruzimuradov O, Nurmanov S, Hojamberdiev M, Prasad RM, Gurlo A, Broetz J, Nakanishi K, Riedel R (2014) Fabrication of nitrogen-doped TiO_2 monolith with well-defined macroporous and bicrystalline framework and its photocatalytic performance under visible light. J Eur Ceram Soc 34:809–816
16. Shi YY, Yang ZW, Wang B, An H, Chen ZZ, Cui H (2016) Adsorption and photocatalytic degradation of tetracycline hydrochloride using a palygorskite-supported Cu_2O–TiO_2 composite. Appl Clay Sci 119:311–320
17. Belver C, Bedia J, Rodriguez JJ (2017) Zr-doped TiO_2 supported on delaminated clay materials for solar photocatalytic treatment of emerging pollutants. J Hazard Mater 322:233–242
18. Karamanis D, Ökte AN, Vardoulakis E, Vaimakis T (2011) Water vapor adsorption and photocatalytic pollutant degradation with TiO_2–sepiolite nanocomposites. Appl Clay Sci 53:181–187
19. Kibanova D, Trejo M, Destaillats H, Cervini-Silva J (2008) Synthesis of hectorite–TiO_2 and kaolinite–TiO_2 nanocomposites with photocatalytic activity for the degradation of model air pollutants. Appl Clay Sci 42:563–568
20. Hu PW, Yang HM, Ouyang J (2012) Synthesis and characterization of Sb–SnO_2 /kaolinites nanoparticles. Appl Clay Sci 55:151–157
21. Zhang YL, Gan HH, Zhang GK (2011) A novel mixed-phase TiO_2/kaolinite composites and their photocatalytic activity for degradation of organic contaminants. Chem Eng J 172:936–943
22. Wang C, Shi HS, Zhang P, Li Y (2011) Synthesis and characterization of kaolinite/TiO_2 nano-photocatalysts. Appl Clay Sci 53:646–649
23. Meenakshi S, Sairam Sundaram C, Sukumar R (2008) Enhanced fluoride sorption by mechanochemically activated kaolinites. J Hazard Mater 153:164–172
24. Chen DM, Zhu Q, Zhou FS, Deng XT, Li FT (2012) Synthesis and photocatalytic performances of the TiO_2 pillared montmorillonite. J Hazard Mater 235–236:186–193
25. Li XG, Liu QF, Cheng HF, Zhang S, Frost RL (2015) Mechanism of kaolinite sheets curling via the intercalation and delamination process. J Colloid Interf Sci 444:74–80
26. Táborosi A, Szilágyi RK (2016) Behaviour of the surface hydroxide groups of exfoliated kaolinite in the gas phase and during water adsorption. Dalton Trans 45:2523–2535
27. Xu HL, Jin XZ, Chen P, Shao G, Wang HL, Chen DL, Lu HX, Zhang R (2015) Preparation of kaolinite nanotubes by a solvothermal method. Ceram Int 41:6463–6469
28. Abou-El-Sherbini KS, Elzahany EAM, Wahba MA, Drweesh SA, Youssef NS (2017) Evaluation of some intercalation methods of dimethylsulphoxide onto HCl-treated and untreated Egyptian kaolinite. Appl Clay Sci 137:33–42
29. Zhang XJ, Liu H, Xing HX, Li HY, Hu HY, Li AJ, Yao H (2017) Improved sodium adsorption by modified kaolinite at high temperature using intercalation-exfoliation method. Fuel 191:198–203
30. Silva ACD, Ciuffi KJ, Reis MJD, Calefi PS, Faria EHD (2016) Influence of physical/chemical treatments to delamination of nanohybrid kaolinite-dipicolinate. Appl Clay Sci 126:251–258
31. Belver C, Vicente MA (2002) Chemical activation of a kaolinite under acid and alkaline conditions. Chem Mater 14:2033–2043

32. Steudel A, Batenburg LF, Fischer HR, Weidler PG, Emmerich K (2009) Alteration of non-swelling clay minerals and magadiite by acid activation. Appl Clay Sci 44:95–104
33. Zhang CY, Zhang ZJ, Tan Y, Zhong MF (2016) The effect of citric acid on the kaolin activation and mullite formation. Ceram Int 43:1466–1471
34. Xu HL, Wang M, Liu QF, Chen DL, Wang HL, Yang KJ, Lu HX, Zhang R, Guan SK (2011) Stability of the compounds obtained by intercalating potassium acetate molecules into kaolinite from coal measures. J Phys Chem Solids 72:24–28
35. Wada K (1965) Intercalation of water in kaolin minerals. Am Mineral 50:924–941
36. Valášková M, Rieder M, Matějka V, Čapková P, Slíva A (2007) Exfoliation/delamination of kaolinite by low-temperature washing of kaolinite–urea intercalates. Appl Clay Sci 35:108–118
37. Bezrodna T, Puchkovska G, Shimanovska V, Chashechnikova I, Khalyavka T, Baran J (2003) Pyridine-TiO_2 surface interaction as a probe for surface active centers analysis. Appl Surf Sci 214:222–231
38. Hajjaji W, Andrejkovičová S, Pullar RC, Tobaldi DM, Lopezgalindo A, Jammousi F, Rocha F, Labrincha JA (2016) Effective removal of anionic and cationic dyes by kaolinite and TiO_2/kaolinite composites. Clay Miner 51:19–27